Effect of Na Substitution on Rare-Earth Manganites

A thesis submitted in the partial fulfilment of the requirement
For the degree of

MASTER OF SCIENCE

IN

PHYSICS

By

Amit sadu Kesarkar

Roll No – 411PH2089

Under guidance of

Dr. Suryanarayan Dash

Dept. of Physics

National Institute of Technology, Rourkela

National Institute of Technology, Rourkela

CERTIFICATE

This is to certify that the thesis entitled "**Effect of sodium substitution on rare earth manganite"** submitted by Mr AMIT SADU KESARKAR in partial fulfilment for the requirement for the award of degree of Master of Science degree in Physics at National Institute of Technology, Rourkela is an authentic work carried out by him under my supervision and guidance in Department of Physics.

To the best of my knowledge, the matter embodied in the thesis has not been submitted to any other University/Institute for the award of any degree or Diploma.

Prof. Suryanarayan Dash
Dept. of Physics
National Institute Technology
Rourkela-769008

ACKNOWLEDGEMENT

On the submission of my thesis report titled "**Effect of Sodium Substitution on Rare Earth Manganite** " I would like to convey my gratitude and sincere thanks to my supervisor Prof. Suryanarayan Dash , Department of Physics for his constant motivation and support during the course of my work in the last one year. I truly appreciate and value his esteemed guidance and encouragement from beginning to the end of this thesis. I am indebted to him for having helped me, shape the problem and providing insights towards the solution. I would like to thank Mr Achyuta Biswal for resistivity measurement of the samples.

Abstract

An effort is made to study the effect of alkali metal substitution in particular Na, on the rare earth side of manganites of La, Nd and Pr. The samples are prepared by wet-chemical route known as Pyrophoric method. The structural characterization of the samples is carried out through detail Reitveld analysis of the XRD data which shows all the samples are single phase and stoichiometric. The granular information and sizes is probed through the SEM analysis. The star like structures of the material is the unique features of samples in the vicinity of the nano order. However the transport properties are unique among the separate constituents of the Na and rare earth combinations starting from pure insulator to metal-insulator transition.

TABLE OF CONTENTS

		Page no.
1.	**INTRODUCTION**	
1.1	Rare Earth Manganite	1
1.2	Properties of manganite	2
1.2.1	Colossal Magnetoresistance	2
1.2.2	Charge ordering	3
1.2.3	Metal-Insulator Transition	3
1.2.4	Phase separation	4
1.3	Manganite with Half doping	5
1.4	Alkali Metal Substitution in Manganite	6
1.5	Aim of the present work	7
2.	**SAMPLE PREPARATION**	8
2.1	Solid state route	8
2.1.1	Calcination	8
2.1.2	Pelletisation	8
2.1.3	Sintering	9
2.2	Wet chemical route	9
2.2.1	Preparation of $Pr_{0.75}Na_{0.25}MnO_3$	10
2.2.2	Preparation of $Nd_{0.75}Na_{0.25}MnO_3$	12
2.2.3	Preparation of $La_{0.75}Na_{0.25}MnO_3$	12
3.	**CHARACTERIZATION TECHNIQUE**	14
3.1	X-ray Diffraction(XRD) and Reitveld Analysis	14
3.2	Scanning Electron Microscope	15
3.3	Resistivity Measurement by 4-probe method	16
4.	**RESULTS AND DISCUSSION**	18
4.1	XRD analysis	18
4.2	SEM image analysis	21
4.3	Resistivity	22
5.	**CONCLUSION and Scope of Future work**	24

REFERENCES

Chapter-1 Introduction

1.1 Rear Earth Manganite:

Manganite is a mineral, its composition is mainly MnO. These manganese based oxide materials, known as manganite , possess unique intrinsic properties of change in electrical resistance under the application of magnetic field, known as magnetoressistance can be expressed as

$$MR\% = \frac{(\rho_0 - \rho_H)}{\rho_0} \times 100$$

Where ρ_0 and ρ_H are the resistivity's in the absence and presence of magnetic field respectively. The doped $LnAMnO_3$ type or better known as ABO_3 type perovskite structure has cubic unit cell, where Ln represents the rare earth elements [1]. At the corner, Mn ions are surrounded by octahedral oxygen units known as the MnO_6 octahedral.

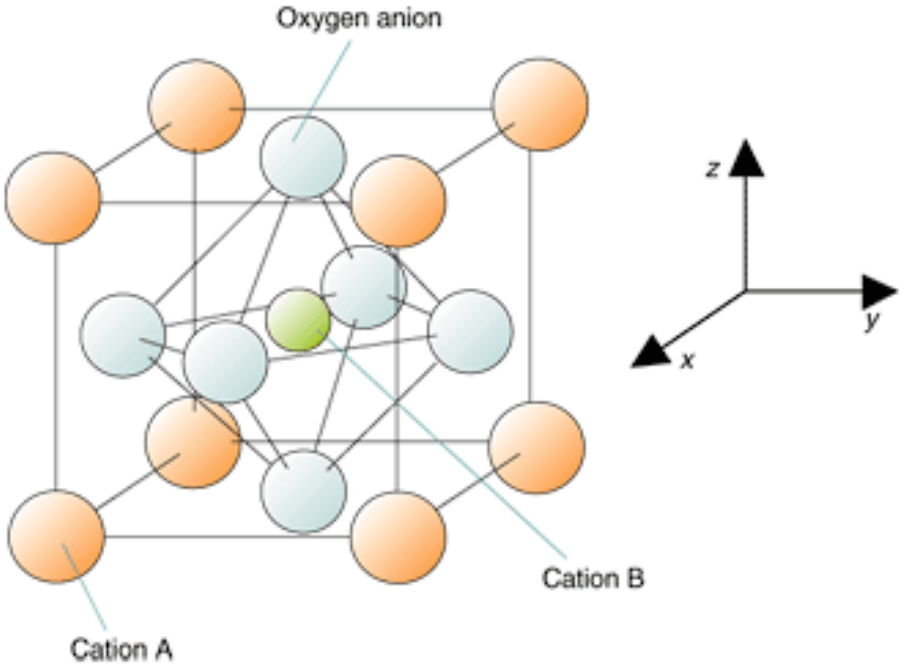

Fig. 1.1: Schematic diagram of perovskite (ABO_3) type structure of manganites.

The relative ion size requirements for stability of the cubic structures are quite stringent, so slight buckling and distortion of MnO_6 octahedral can produce several low-Symmetry distorted structures, in which co-ordinate number of Ln cations and Mn or both is reduced. Complex perovskites structures contain two different Mn-sites cations (Mn^{3+} and Mn^{4+})[1]. This results in possibility of ordered and disordered structures. The orthorhombic and tetragonal phases are most commonly observed non-cubic structure for doped manganite. The factors affecting most of its physical properties includes $<r_A>$ = the Average A site ionic radii, t = tolerance factor is an indicator for the stability and distortion of crystal structure $t = \frac{r_A + r_o}{\sqrt{2}\,(r_B + r_o)}$ Where r_A is the radius of A cation, r_B is the radius of B cation, r_o is the radius of anion respectively, and the variances namely σ^2 [1].

1.2 Properties of Manganites:

The rare earth managnites is well known for their intrinsic but interesting physical phenomena and many researchers studied such class of materials for several decades. Some important properties includes colossal magnetoresistance, Double exchange, phase separation, orbital and charge ordering etc [1].

1.2.1 Colossal Magneto Resistance (CMR):

Colossal Magneto resistance is a property of some materials, mostly manganese based perovskite oxides that enables them to dramatically change their electrical resistance in presence of magnetic field. The magneto resistance of conventional materials enables changes in resistance of up to 5% but materials featuring CMR may demonstrate resistance changes by orders of magnitude. The magneto resistance, that means the resistance change induced by an external magnetic field, these phenomena observed, more or less in all metals and semiconductors. The particular MR phenomena to be described here are the

gigantic decrease of resistance by application of magnetic field that is observed for the transition metal oxides and arise from the spin dependent scattering process of the conduction electron. Importantly the local spin and conduction electron are both of d-electron character. The external magnetic field cause the gigantic decrease of the resistivity around the curie temperature of that compound, below which the resistivity also show a steep decrease with decreasing temperature in zero field. Such gigantic negative magnetoresistance is called as colossal mangneto-resistance [1,2,3]. Many of the functional properties of these materials can be identified by this property.

1.2.2 Charge Ordering:

Charge ordering refers to the ordering of the metal ions in different oxidation states in specific lattice sites of mixed valent material[2]. Such ordering genrally localizes the electrons in the materials, making it insulating or semiconducting due to charge localization witch in turns restricts the electron hoping form one cation site to another. Charge ordering is not a new phenomenon in metal oxides.

In doped manganites, the charged-ordered phases are novel manifestation arising from the interaction between the charge carriers and the phonons where in the jahn Teller distortion play a significant role. Charge ordering arises because the carriers are localized into specific sites below certain temperatures know as charge ordering temperature.

1.2.3 Metal-Insulator Transition:

Metal–insulator transitions are transitions from a metal to an insulator material where conductivity of charges is quickly suppressed. These transitions can be achieved by tuning various ambient parameters such as pressure or, in case of a semiconductor, doping.

The classical band structure of solid state physics predicts the Fermi level to lie in a band gap for insulators and in the conduction band for metals, which means metallic behavior is seen for compounds with partially filled bands. However, some compounds have been found which show insulating behavior even for partially filled bands. This is due to the electron-electron correlation, since electrons can't be seen as noninteracting. Mott considers a lattice model with just one electron per site. Without taking the interaction into account, each site could be occupied by two electrons, one with spin up and one with spin down. Due to the interaction the electrons would then feel a strong Coulomb repulsion, which Mott argued splits the band in two: The lower band is then occupied by the first electron per site, the upper by the second. If each site is only occupied by a single electron the lower band is completely filled and the upper band completely empty, the system thus a so called Mott insulator[1,2,3].

1.2.4 Phase Separation:

Mixed valent manganites show a great deal of fascinating properties, arising from the strong interplay between spin, charge, orbital and lattice degrees of freedom. The most intriguing one is the existence of phase separated state where the submicrometer size ferromagnetic (FM) - metallic (M) and antiferromagnetic (AF) - insulating (I) phases simultaneously and spontaneously coexist [3]. Though initially this observation was ascribed to the bad quality of materials but now it is apparent that this phase inhomogeneity is intrinsic to the system, and has been observed even in purest form of single crystals. This observed inhomogeneity, which is usually referred as phase separation (PS), has been accepted as crucial in explaining various complex phenomenon in transition metal oxides like, manganites, cuprates and nickelates. This phase inhomogeneity has been argued as the essential ingredient for colossal magnetoresistance properties, and considered as a inherent feature for bicritical phase competition in manganites. Despite of a considerable amount of efforts,

involving both theories and experiments, the origin of PS is not clear. It is commonly believed that PS scenario has its origin in the unusual proximity of free energies of these very distinct FM and AF phases and the com- petition between both the phases is resolved in giving rise to real-space inhomogeneities in the materials. However, there exists debate related to size as well as nature of the coexisting phases. Theoretical calculation have shown that density of eg electrons changes discontinuously when chemical potential μ was varied indicating that ground state is not homogeneous but is separated into two regions with different electronic densities. This situation gives rise to nanoscopic electronic PS, as the micrometer size PS of two phases with unequal electronic density will be simply prevented by the long-range Coulombic repulsion which breaks the large clusters into small pieces and tries to spread the charges more uniformly. This provides a stable situation which is energetically more favorable, with one type of clusters embedded into other phase[3].

1.3 Manganites with Half Doping:

Perovskite manganites with 50% of trivalent rare-earth ions of R^{3+} replaced by divalent alkaline-earth metal ions of A^{2+}, $R_{0.5}A_{0.5}MnO_3$ (R=La, Pr, Nd, etc; A=Sr, Ca) known as half doped manganites, have been extensively studied and found to show many interesting electronic and magnetic properties. There are metal(M)-insulator(I) transition due to the double-exchange interaction (magnetic interaction between Mn^{3+} and Mn^{4+} that is caused by the hopping of eg electrons between the two partially filled d shells with strong on-site Hund's coupling), charge-ordering (CO) transitions due to the long-range Coulomb interaction among the carriers and antiferromagnetic transition due to the super exchange interaction, depending on the combination of R and A atoms. The above properties of manganites investigated, have been discussed by using various parameters such as average ionic radii $<r_A>$ of R^{3+} and A^{2+}, tolerance

factor t (which is a geometrical index defined as $t = (r_A+r_O)/2(r_{Mn}+r_O)$, where r_O is the ionic radius of O^{2-} and r_{Mn} is the average ionic radius of Mn^{3+} and Mn^{4+}), variance σ^2 etc. The 50% doping of the divalent metal cation on the rare earth site results a mixed valence with equal proportions of Mn^{3+} and Mn^{4+} ions in the system. From these classes, $La_{0.5}Sr_{0.5}MnO_3$ and $Pr_{0.5}Sr_{0.5}MnO_3$ compound with a larger $<r_A>$, shows the metallic conductivity and a layered A-type AFM state where as $Nd_{0.5}Ca_{0.5}MnO_3$, $Pr_{0.5}Ca_{0.5}MnO_3$, $La_{0.5}Ca_{0.5}MnO_3$, and $Nd_{0.5}Sr_{0.5}MnO_3$ etc with a smaller $<r_A>$, a CO insulating ground state has been obtained, in which Mn^{3+} and Mn^{4+} ions form two sublattice charge-exchange (CE)-type AFM structure. However, recently, the similar class of materials has been obtained by substituting a lower fraction of monovalent/alkali metal cation (Na^+, K^+ etc) on the same rare earth site. Due to charge neutrality, 25% of such alkali metal ion results a mixed valence of Mn^{3+} and Mn^{4+} ions (equal proportion) in the compound. Such mixed valence leads to several interesting properties in this system[1,2,3].

1.4 Alkali metal substitution in manganite:

Most of the studies in recent past based mostly on the divalent metal on the rare earth sides of such manganite which shows many interesting properties. For instance Ca and Sr substitution on rare earth sides not only disturb the parent system structurally but it changes the physical properties also[1]. The magnetic properties changes from antiferromagnetic insulator (parents compounds $LaMnO_3$) to ferromagnetic metallic ($La_{0.5}Sr_{0.5}MnO_3$). Similar phenomena can be expected for alkali metal substitution also. But here the properties can be expected by a lower substitution of such metal, as it is lower by valence one. In this case to have charge neutrality, the lower substitution of Na gives rise to similar hole concentration to the double of their divalent counterpart as Sr and Ca etc[]. In a similar context the controlling parameters for the alkali metal substitution on rare earth elements of the managnites as follows;

Manganites	$<r_A>$	σ^2	t
$Pr_{0.75}Na_{0.25}MnO_3$	1.315	1.875×10^{-3}	0.9659
$Nd_{0.75}Na_{0.25}MnO_3$	1.300	2.7×10^{-3}	0.9605
$La_{0.75}Na_{0.25}MnO_3$	1.367	0.168×10^{-3}	0.9846

The symbols are their usual meaning as discussed in the previous sections. The ionic radii are taken from the data given in reference 1.

1.5 Aim of the Present Work:

An effort is made to study the effect of alkali metal substitution in particular Na, on the rare earth side of manganites of La, Nd and Pr and their physical properties. The samples are prepared by wet-chemical route known as Pyrophoric method which is unique in their first preparation process. The structural characterization of the samples is carried out through detail Reitveld analysis of the XRD data which shows all the samples are single phase and stoichiometric. The granular information and sizes is probed through the SEM analysis. The star like structures of the material is the unique features of samples in the vicinity of the nano order. However the transport properties are unique among the separate constituents of the Na and rare earth combinations starting from pure insulator to metal-insulator transition.

Chapter-2 Sample Preparation

Usually many of the compounds are synthesized mainly either by solid state reaction route or wet-chemical mixing route in condensed mater physics.

2.1 Solid state route:

This preparation method is mostly followed in preparaing the ceramic materials. It a process of direct mixing of the constituent powders in a stoichiometric ratios and heat treatment is given to the samples with intermediate grinding. During the process of preparation, it undergoes few intermediate processes; includes calcinations, pelletization, sintering etc [4].

2.1.1 Calcination:

Calcination is a thermal treatment process in presence of air applied to ores and other solid materials to bring about a thermal decomposition phase transition or removal of a volatile fraction. The calcination processes normally take place below the melting point of the product materials. Calcination is to be distinguished from roasting, in which more complex gas solid reaction take place between the furnace atmospheres of the solid.

The calcination reaction usually takes place at or above the thermal decomposition or transition temp. This temp is usually defined as the temp at whom the standard Gibbs free energy for a particular calcination reaction is zero [4].

2.1.2 Pelletisation:

It is process of pressing the powder in uni-axial die press at room temp by applying a force on it for increasing reaction rate. Here we have to increase area of contact between the particles, this can be achieved by pressing the reaction

powder into pellets but even at high pressure the pellets are usually porous and the crystal contacts are not maximized. Typically cold pressed pellets are 20% to 40% porous. Depending upon requirement of our sample formation, sometimes hot press is required. So that combined effect of temp and pressing may cause the particle to fit together better but densification process is usually slow and may require several hours [4].

2.1.3 Sintering:

It is a method to create objects from powder. It is based on atomic diffusion principle. Diffusion occurs in many materials above absolute zero, but it occurs much faster at higher temp. In most sintering process, the powdered materials is held in mold and then heated to a temp below the melting point. The atoms in the powder particles diffuse across boundaries of the particle, fusing the particle together and creating one solid piece [4].

2.2 Wet Chemical route:

As alkali metal is volatile, we have opted the second route as it needs low sintering temperature and time. In this project we will prepared mostly Na metal substitution in three different rare earth (Pr, Nd and La) manganites around half doping.

Pyrophoric technique

It is a popular wet chemical route for fabrication of materials, favourably metal oxides. In this method aqueous solution of the requisite amount of ingredient materials are taken in stoichiometric proportion. The individual solution is heated up and concentric HNO_3 is added drop wise until it become clear then triethanolamine(TEA) is added with these solutions in such way that metal ions to TEA ratio is maintained at 1:1:2 to make a viscous solution. The clear solution of TEA complexed metal nitrates was evaporated around 200^0 C with constant stirring. The continuous heating of these solutions causes foaming and puffing. During evaporation the nitrate ions provides an in situ oxidization

environment for TEA, which partially converts the hydroxyl group of TEA into carboxylic acid. When complete dehydration occurs, the nitrate themselves are decomposed with the evolution of brown fumes of NO_2 leaving behind a voluminous, organic based black fluffy powder. i.e. precursor powder. The precursor powder after proper grinding are calcined at various temp to get the desired compound with variable particle size [5].

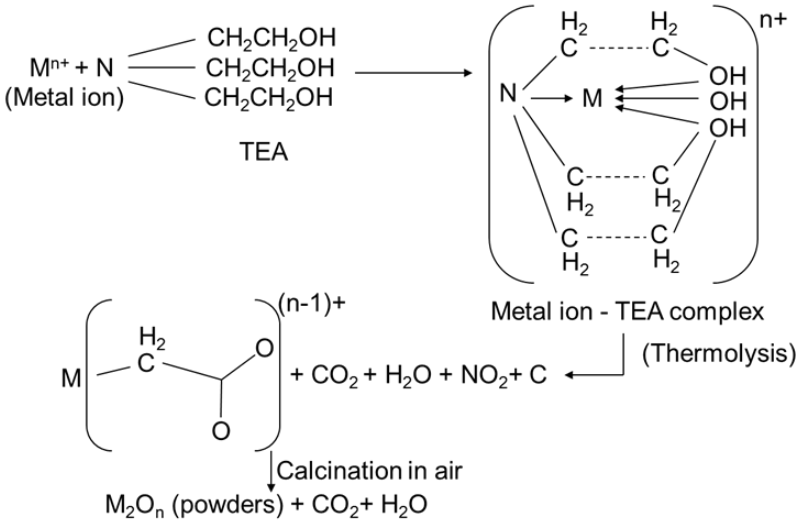

Fig. 2.1: Schematic of chemical reaction of TEA in formation of the compounds

2.2.1 Preparation of $Pr_{0.75}Na_{0.25}MnO_3$

Calculation for synthesis of 5 grams of $Pr_{0.75}Na_{0.25}MnO_3$ by pyrophoric process.

Table 2.1:

Starting material	Mol wt. (gm.)	Wt. required of necessary moles component	Wt. required for initial compound of 5 gm. of assumed compound
Pr_6O_{11}	**1021.442**	**127.768**	**1.6209**

Na(NO_3)	**84.995**	**21.248**	**0.2695**
Mn.Acetate	**245.09**	**245.09**	**3.1094**
		Total= 394.106	

Mole required quantity of starting materials:

Pr_6O_{11} = 0.009514 moles; Na (NO_3) = 0.003170 moles; Mn.Accetate= 0.02537 moles. So Required TEA = 7.56990 ml

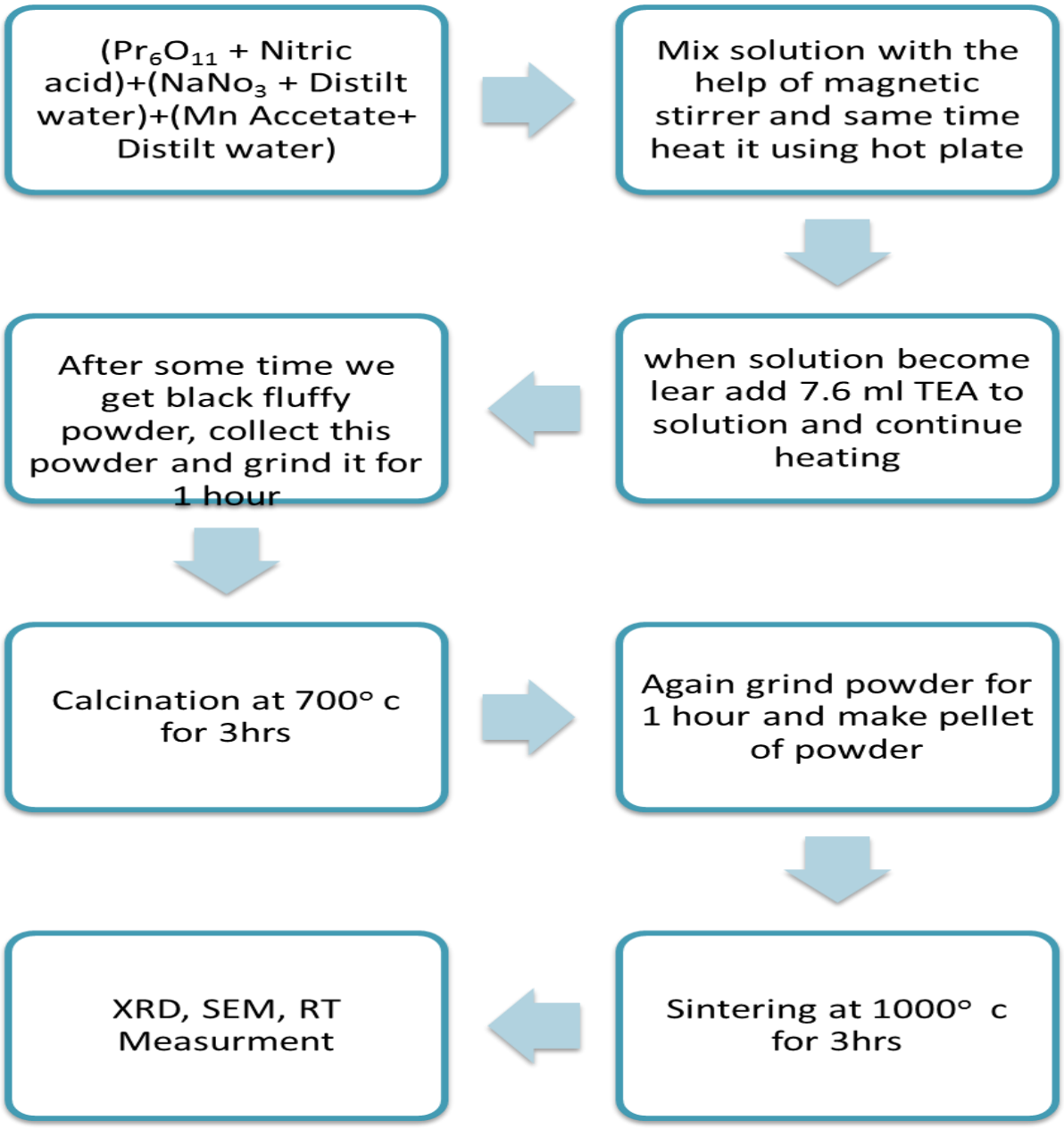

2.2.2 Preparation of $Nd_{0.75}Na_{0.25}MnO_3$

Calculation for synthesis of 5 grams of $Nd_{0.75}Na_{0.25}MnO_3$ by pyrophoric process.

starting material	Mol wt. (gm.)	Wt. required of necessary moles component	Wt. required for initial compound of 5 gm. of assumed compound
Nd_2O_3	**336.48**	**126.18**	**1.6073**
Na(NO_3)	**84.995**	**21.247**	**0.2706**
Mn.Acetate	**245.09**	**245.09**	**3.1220**
		Total= 392.517	

Table 2.2:

Mole required quantity of starting materials:

Nd_2O_3 = 0.009553 moles; Na (NO_3) = 0.003183 moles; Mn.Accetate= 0.01273 moles; So Required TEA = 7.5967 ml

Similar procedure has been followed like the above material preparation.

2.2.3 Preparation of $La_{0.75}Na_{0.25}MnO_3$

Calculation for synthesis of 5 grams of $La_{0.75}Na_{0.25}MnO_3$ by pyrophoric process. Table 2.3:

tarting material	Mol wt. (gm.)	Wt. required of necessary moles component	Wt. required for initial compound of 5 gm. of assumed compound
La_2O_3	**325.82**	**122.18**	**1.5723**

$Na(NO_3)$	**84.995**	**21.247**	**0.2734**
Mn.Acetate	**245.09**	**245.09**	**3.1541**
		Total= 388.517	

Mole required quantity of starting materials:

La_2O_3 = 0.009651 moles; Na (NO_3) = 0.003216 moles; Mn.Accetate= 0.01286 moles; so require amount of TEA = 7.6764 ml

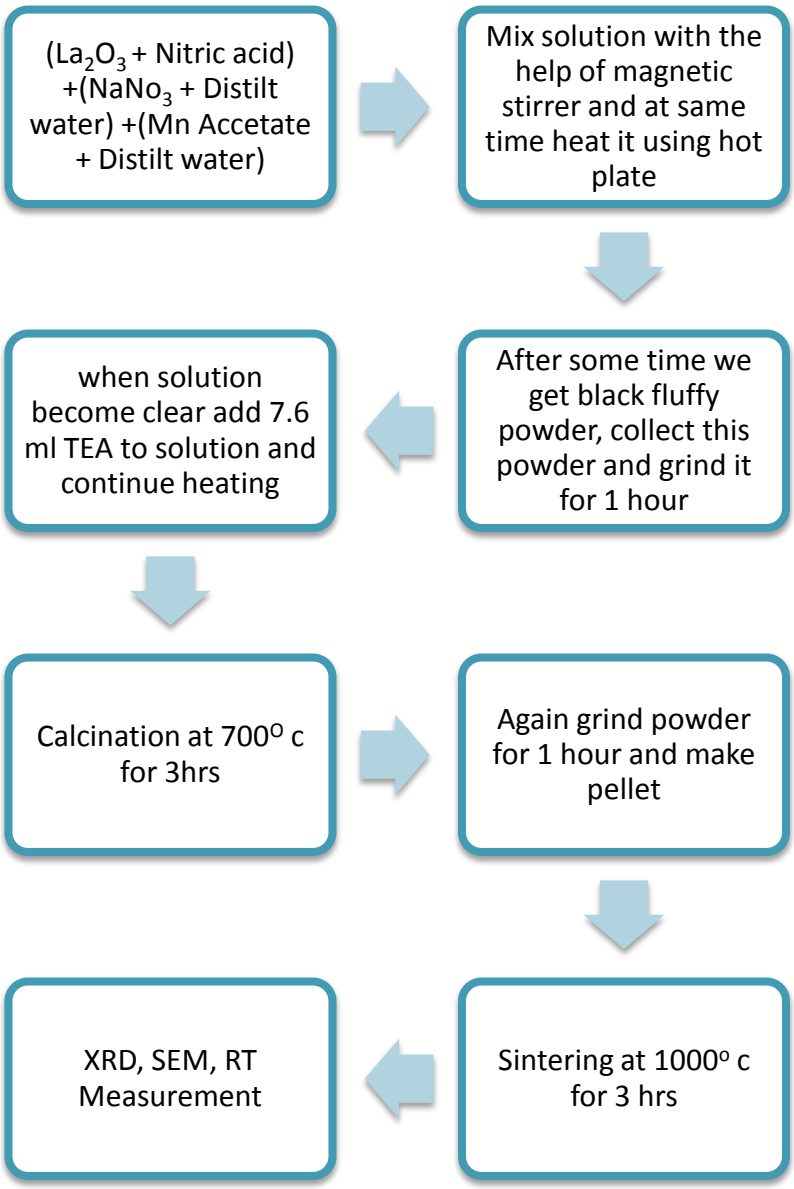

Chapter-3 Characterization Techniques

3.1 X-ray Diffraction and Reitveld Analysis:

XRD is most common technique for the study of crystal structure and atomic spacing. It is also used for the identification of phase of a crystalline material and also provides information on unit cell dimensions. It is based on the principle of interference. X-ray diffraction occurs when there is a constructive interference between the monochromatic x-rays and the crystalline sample.

X-rays to be used are generated by a cathode ray tube by heating a filament to produce electrons. These electrons are then accelerated with the help of an applied voltage towards the target material. There are two types of X-ray depend upon how accelerated electron interacts with target material, and those are characteristic spectra and continuous spectra. In X-ray diffraction we use characteristic spectra; Cu-kα is widely used in XRD. In this case the diffraction occurs for the plane for which satisfies the Bragg's diffraction condition as $2d \sin\theta = n\lambda$

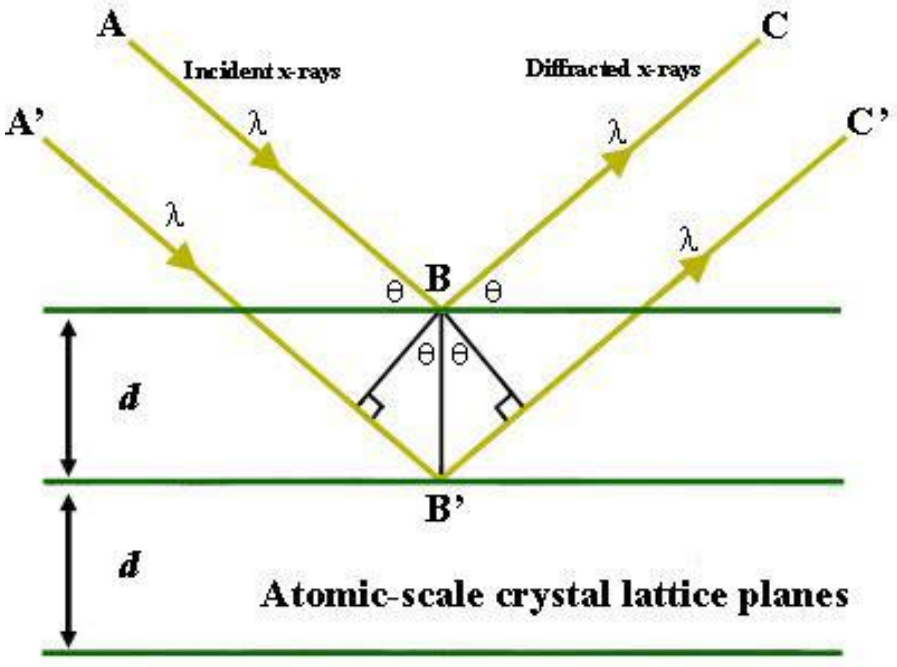

Fig 3.1The schematic representation of the XRD. The symbols used in the schematic are their usual meaning.

Rietveld refinement/Analysis is a technique devised by Hugo Rietveld for use in the characterisation of crystalline materials. The neutron and x-ray diffraction of powder samples results in a pattern characterised by reflections (peaks in intensity) at certain positions. The height, width and position of these reflections can be used to determine many aspects of the materials structure.

The Rietveld method uses a least squares approach to refine a theoretical line profile until it matches the measured profile (xrd data from the diffractometer). The introduction of this technique was a significant step forward in the diffraction analysis of powder samples as, unlike other techniques at that time; it was able to deal reliably with strongly overlapping reflections [6].

3.2 Scanning Electron Microscope imaging:

A SEM is a type of electron microscope that produces images of a sample by scanning it with a focused beam of electrons. The electrons interact with electrons in the sample, producing various signals that can be detected and that contain information about the sample's surface topography and composition. The electron beam is generally scanned in a raster scan pattern, and the beam's position is combined with the detected signal to produce an image. SEM can achieve resolution better than 1 nanometer. Specimens can be observed in high vacuum, low vacuum and in environmental SEM specimens can be observed in wet conditions.

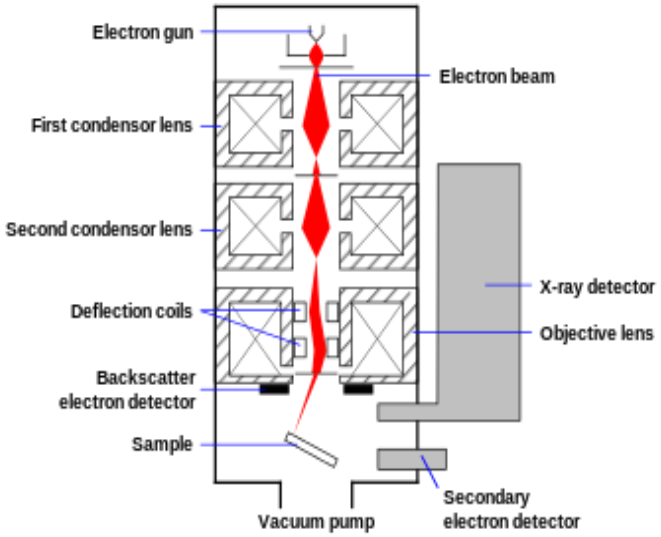

Fig3.2 Scematic representation of SEM used in this work

In the most common or standard detection mode, secondary electron imaging or SEI, the SEM can produce very high-resolution images of a sample surface, revealing details less than 1 nm in size. Due to the very narrow electron beam, SEM micrographs have a large depth of field yielding a characteristic three-dimensional appearance useful for understanding the surface structure of a sample. This is exemplified by the micrograph of pollen shown above. A wide range of magnifications is possible, from about 10 times (about equivalent to that of a powerful hand-lens) to more than 500,000 times, about 250 times the magnification limit of the best light microscopes. The SEM used in this work belongs to JSM 6480 LV-JEOL microscope [6].

3.3 Resistivity Measurement by four probe method:

Typically in most cases the resistivity of the specimen is measured by 4-probe method for better accuracy.

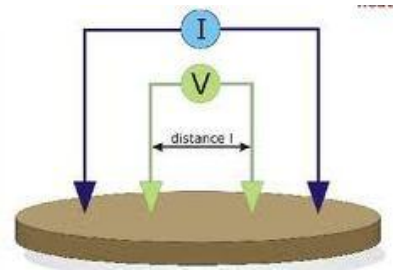

Fig3.3 Schematic diagram of the 4-probe method of resistivity measurement.

The four-point probe consists of four equally spaced metal tips with finite radius. A high impedance current source is used to supply current through the two outer probes, while a voltmeter measures the voltage drops across the inner two probes to determine the sample resistivity [6]. Typical probe spacing ~ 1mm. The temperature dependence of the resistivity is measured in a closed cycle refrigerator with temperature insert for varying temperatures.

Chapter-4 Results and Discussions

4.1 Structural analysis by XRD

The XRD pattern of the $Pr_{0.75}Na_{0.25}MnO_3$ is shown in fig4.1. The structural characterization of the samples was carried out by powder x-ray diffraction (XRD) using Phillips PW 1830 HT X-ray generator.

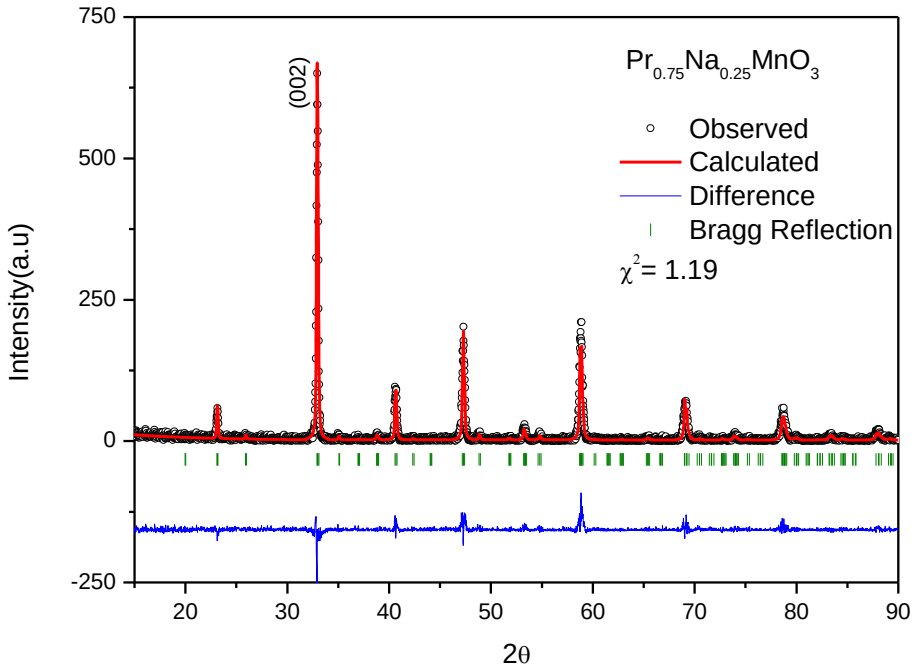

Fig 4.1: Reitveld analysis of X-ray diffraction pattern for $Pr_{0.75}Na_{0.25}MnO_3$.

It can be seen from the figure that sample is in single phase with orthrombic perovskite structure and Pnma space group [7,8]. The cell parameters of all the samples are obtained by refining the experimental data using a standard Rietveld refinement technique with a good-ness-fit value(χ^2).

Refined structural parameters of $Pr_{0.75}Na_{0.25}MnO_3$ (S.G: P n m a)

Atoms	x	y	z
Pr	0.0202(6)	0.25	0.0016(1)
Na	0.0202(6)	0.25	0.0016(1)
Mn	0	0	0.5

O_1	0.5048(6)	0.25	0.0628(1)
O_2	0.2720(7)	0.0409(2)	0.7403(9)

a = 5.4229(5); b = 7.6963(7); c = 5.4405(5)

R_p = 39.9; R_{wp} = 44.5; R_{exp} = 41.49

Bragg R-factor = 14.80

R_F factor = 11.05

χ^2 = 1.19

The XRD pattern of the $Nd_{0.75}Na_{0.25}MnO_3$ is shown in fig4.2

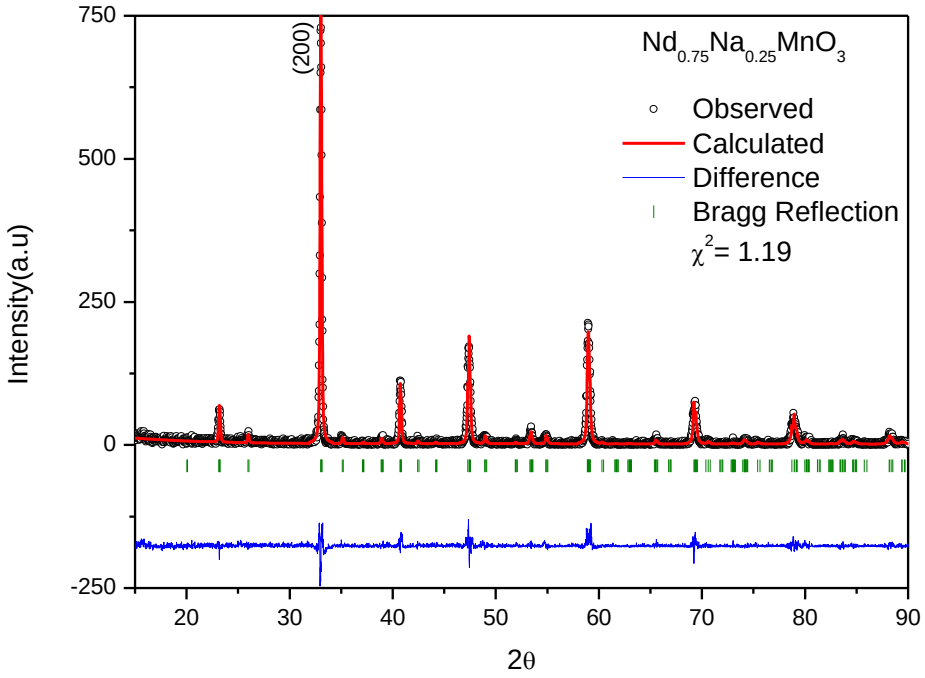

Fig 4.2: Reitveld analysis of X-ray diffraction pattern for $Nd_{0.75}Na_{0.25}MnO_3$.

Refined structural parameters $Nd_{0.75}Na_{0.25}MnO_3$ (S.G: P n m a) ,matches well with reference 9.

Atoms	x	y	z
Nd	0.0264(5)	0.25	-0.0038(2)
Na	0.0264(5)	0.25	-0.0038(2)
Mn	0	0	0.5
O_1	0.4974(5)	0.25	0.0787(11)
O_2	0.2826(8)	0.0283(5)	0.7223(9)

a = 5.4144(6); b = 7.6836(6); c = 5.4203(6)

R_p = 35.8; R_{wp} = 43; R_{exp} = 39.58; Bragg R-factor = 8.558; R_F factor = 7.498; χ^2 = 1.19

The XRD pattern of the $La_{0.75}Na_{0.25}MnO_3$ is shown in fig4.3

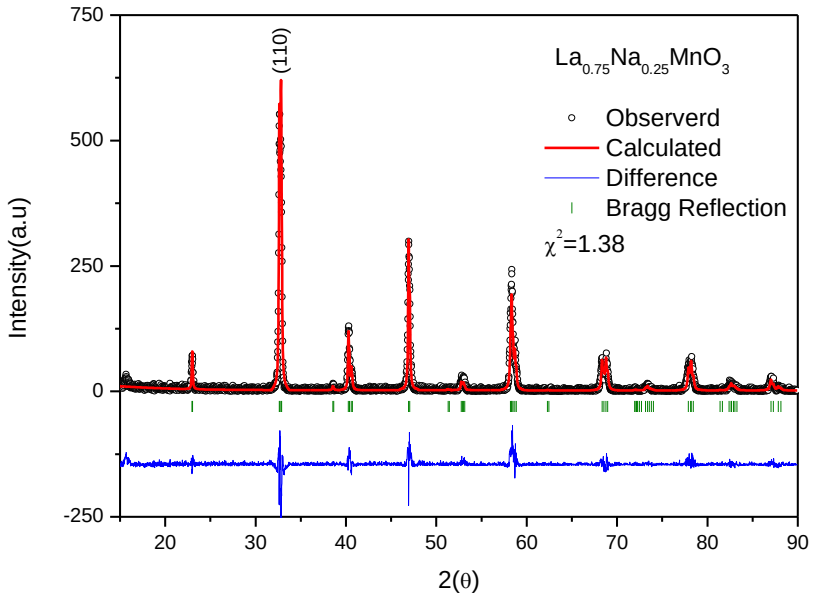

Fig 4.3: Reitveld analysis of X-ray difffraction pattern for $La_{0.75}Na_{0.25}MnO_3$.

It can be seen from the figure that sample is in single phase with rhombohedral perovskite structure and $R\bar{3}c$ space group in which La/Na atoms are the cell parameters of all the samples are obtained by refining the experimental data using a standard Rietveld refinement technique [10].

Refined structural parameters $La_{0.75}Na_{0.25}MnO_3$ (S.G: $R\bar{3}$ C)

Atoms	x	y	z
La	0	0	0.25
Na	0	0	0.25
Mn	0	0	0.5
O	0.4594(3)	0	0.25

a = 5.4859(4); b = 5.4859(4); c = 13.3250(1)

R_p = 36.3; R_{wp} = 41.6; R_{exp} = 35.42

Bragg R-factor = 12.22

R_F factor = 7.64

χ^2 = 1.38

From the above analysis we found that all the samples are single phase and stoichiometric with their respective space groups.

4.2 SEM analysis:

The SEM image of the materials has been obtained from JSM 6480 LV-JEOL microscope. Fig4.4 and 4.5 shows the image of $Pr_{0.75}Na_{0.25}MnO_3$ and $Nd_{0.75}Na_{0.25}MnO_3$ in various magnification respectively. The as prepared samples are at low sintering temperature and time, initial imaging shows some star like shape at the surface level as expected and similar shape to a nano form.

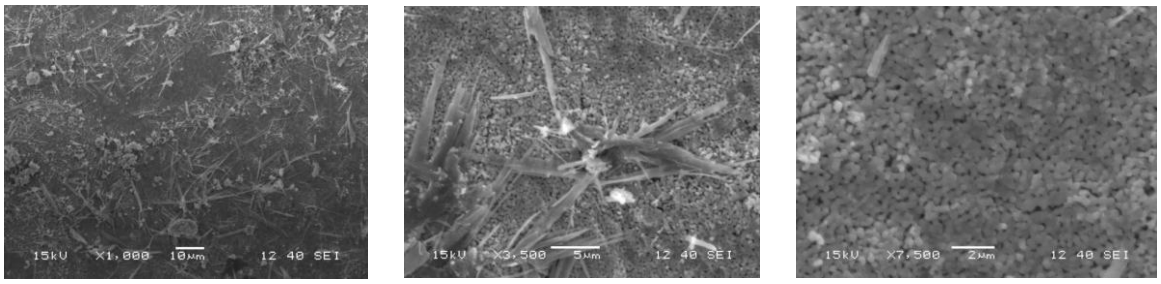

Fig4.4 SEM image of $Pr_{0.75}Na_{0.25}MnO_3$

Similar but distinguishable features are also seen in other samples too. With further magnification one can see the formation of grains although it is not so clear.

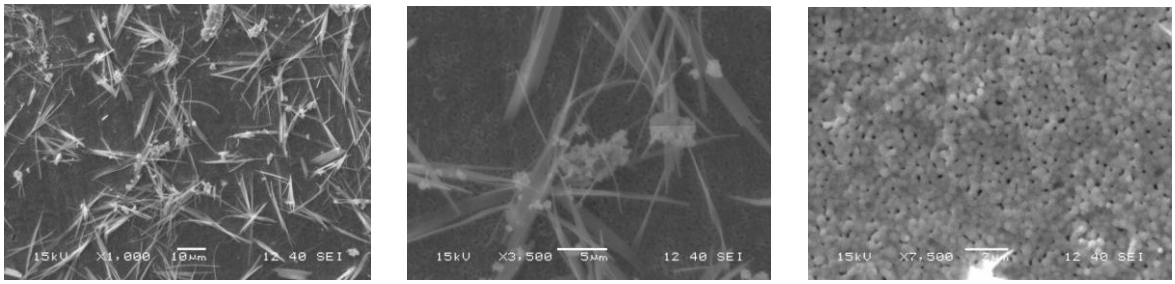

Fig4.5 SEM pictures of $Nd_{0.75}Na_{0.25}MnO_3$

Most prominent image with similar star like structure with lower magnifications is shwin in fig4.6. It is either due to noano size formation of the materials or may be from the clusters of foreign particles on the surface of the materials.

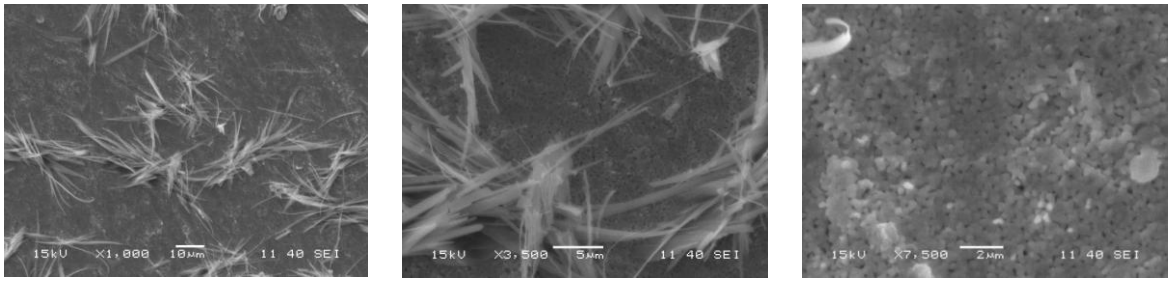

Fig4.6 SEM image of $La_{0.75}Na_{0.25}MnO_3$ with different magnifications

4.3 Temperature dependence of resistivity:

To study the transport properties of the materials with Na composition in rare earth side of manganites, and its effect, resistivity is measured as a function of temperature for all three materials.

Fig4.7 shows zero field R vs T for $Pr_{0.75}Na_{0.25}MnO_3$. At room temperature we expect the Mn ions are at random. While cooling the samples the resistivity undergoes a step rise at T_{CO} around 220K[7,8], which shows charge ordering in which the constituents Mn^{3+} and Mn^{4+} are ordered. With further lowering of T, the resistivity rises exponentially and becomes above the measurement limit of the instruments, which characterises highly insulating behaviour of the material.

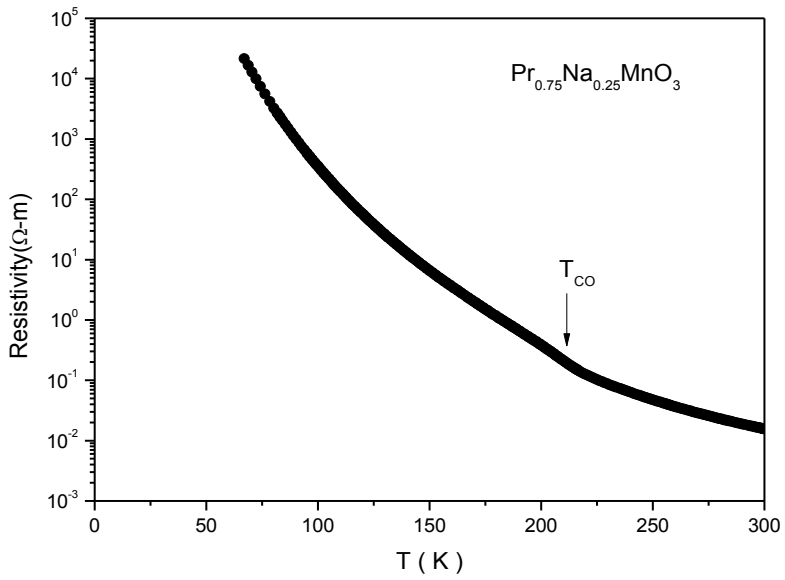

Fig4.7 Resistance vs. Temp curve of $Pr_{0.75}Na_{0.25}MnO_3$

Similar but slightly different behavior has been observed in Nd case. With lowering temperature, resistivity rises with slightly fall below around 200K, but no prominent signature of charge ordering and below that it cannot be measured,. However the resistivity value is lower than that measured in Pr case.

Comparing the tolerance factor, the value for Pr is higher than Nd so tending towards a lower resistivity value [9].

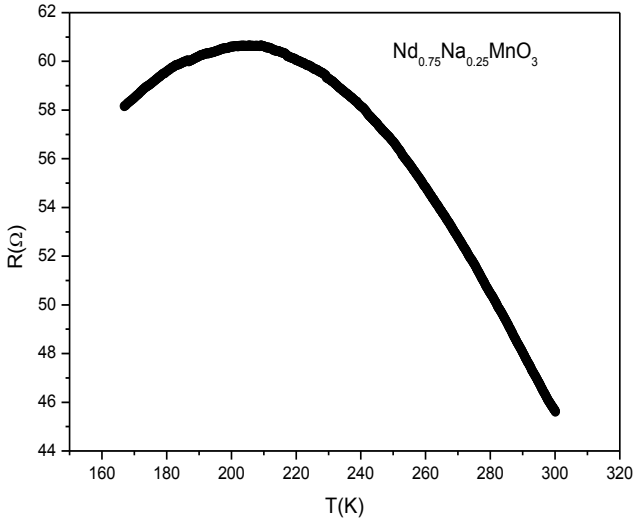

Fig4.8 Resistance vs. Temp curve of $Nd_{0.75}Na_{0.25}MnO_3$

The $La_{0.75}Na_{0.25}MnO_3$ undergoes an insulator to metal transition at around 200K upon lowering of temperature. It may be due to the radii difference of the constituent materials. The Na substitution on La side results an equal concentrations of Mn^{3+} and Mn^{4+}, which may undergoes Double exchange interaction, resulting metallicity along with ferromagnetism [10].

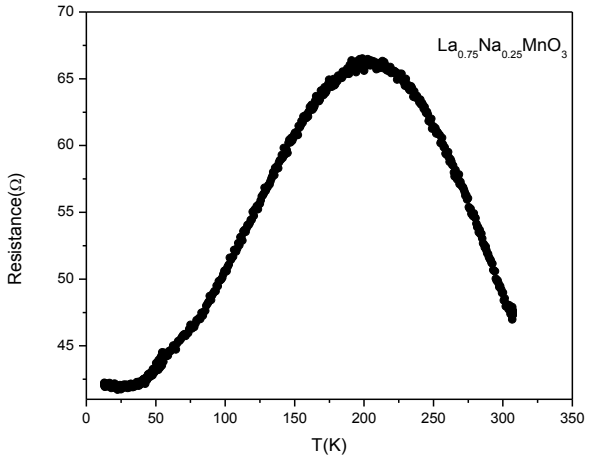

Fig4.9 Resistance vs. Temp curve of $La_{0.75}Na_{0.25}MnO_3$

Chapter-5 Conclusion and Scope of future work

To sum up, the effect of alkali metal substitution in particular Na, on the rare earth side of manganites of La, Nd and Pr has been studied trough detail structural, imaging and transport measurements. The samples are prepared by wet-chemical route known as Pyrophoric method in which a homogeneous materials is obtained along with Na concentration in the materials can be intact without vaporization as the vapour pressure of Na is lower. The structural characterization of the samples is carried out through detail Reitveld analysis of the XRD data which shows all the samples are single phase and stoichiometric. The granular information and sizes is probed through the SEM analysis. The star like structures of the material is the unique features of samples in the vicinity of the nano order. However the transport properties are unique as Na and rare earth combinations starting from pure insulator for Pr case with a prominent charge ordering temperature to semiconducting in Nd and subsequently to an insulator to metal transition in La and Na combinations.

Several scopes has been opened in this field, the detail magnetic measurement can shed light to the internal mechanism for the deviation of the physical properties for similar compositions of Na in different rare earth elements. One can also try the different form of the material like thin film or nano materias and study the properties in detail.

References

1. Y. Tokura, Colossal Magnetoresistive oxides, Gordon and Breach Science publishers
2. C. N. R Rao;' colossal magnetoresistace, charge orsdering and related properties of mananganese oxides" world scientific publishing co.
3. E. Dagotto, 'Nanoscale Phase Separation and Colossal Magnetoresistance', Springer publishers.
4. A. R. West , Solid state chemistry and its applications, John willey sons, Singapore 1887
5. R. K Pati etal, J. Am Cermic Soc, **84**, 2849(2001)
6. www.wikipedia.org
7. S. Dash etal, J. Appl. Phys. **113**, 17D912 (2013)
8. X. H. Zhang etal, Solid State Communi. **135**, 356(2005)
9. Z. Q. Li etal, J. Mag. Mag Mater **284**, 133 (2004)
10. Y. K. Lakshmi etal, J. Appl. Phys **106**, 023707(2009)